Lithium insertion into the raw multi-walled carbon nanotubes pre-doped with lithium - An electrochemical impedance study

ARTICLE *in* DIAMOND AND RELATED MATERIALS · JANUARY 2004

Impact Factor: 1.92 · DOI: 10.1016/j.diamond.2003.09.006

4 AUTHORS, INCLUDING:

Zhanhong Yang
Central South University
59 PUBLICATIONS **482** CITATIONS

SEE PROFILE

Shangbin Sang
Central South University
27 PUBLICATIONS **188** CITATIONS

SEE PROFILE

Available online at www.sciencedirect.com
SCIENCE DIRECT®
Diamond and Related Materials 13 (2004) 99–105
DIAMOND AND RELATED MATERIALS
www.elsevier.com/locate/diamond

Lithium insertion into the raw multi-walled carbon nanotubes pre-doped with lithium—an electrochemical impedance study

Zhanhong Yang[a,*], Shangbin Sang[a], Kelong Huang[a], Hao-qing Wu[b]

[a]*College of chemistry and chemical engineering, Central South University, Changsha 410083, PR China*
[b]*Department of chemistry, Fudan University, Shanghai 200433, PR China*

Received 6 February 2003; received in revised form 1 July 2003; accepted 23 September 2003

Abstract

The raw carbon nanotubes were synthesized by electric arc method and doped with lithium. Electrochemical impedance spectroscopy was applied for the raw carbon nanotubes pre-doped with lithium during Li-ion insertion in the electrolyte of 1 M $LiClO_4$/EC + DMC. After treated with lithium compounds the reversible capacity was increased than that of raw carbon nanotubes. The impedance spectra measured consist of a depressed semicircle in the high frequency range and a straight line at low frequency. Obtained spectroscopies were analyzed with an equivalent circuit model. Kinetic parameters such as the charge transfer resistance and the chemical diffusion coefficient of Li-ion in the carbon nanotubes were evaluated. It showed that the D_{Li} increased as the Li concentration increased. The possible reasons that can explain the variations in the diffusion coefficient with the open circuit voltage are controlled by the effective cross-section of the diffusion.

Keywords: Lithium; Carbon nanotubes; Raw; Dope; Intercalation; Impedance

1. Introduction

In 1990 Sony [1] surprised the 'battery world' by abandoning rechargeable lithium battery development, in which they had been deeply involved for several years with a Li/MnO_2 couple, to introduce a new concept, which they named 'Li-ion'. Based on previous scientific studies and some early prototype results, engineers from Sony were able to demonstrate that disorder non-graphitizable carbons (hard carbon) can insert lithium using appropriate electrolytic solution and a suitable electrode technology. Since this time, a lot of research and development work [2–4] has been increasingly carried on worldwide, and very rapid and significant improvements were made to the insertion materials used in these batteries. For example, crystallized carbons can now be used without exfoliation, bringing useful improvement to cell voltage and energy. Considerable economic incentives linked to the huge development of portable electronic devices such as cellular or notebook computer.

The novel carbon nanomaterial [5] is now attracting great interest with researchers in physics and chemistry as well as materials science [6–9]. Nanotubes exhibit unique physical and chemical properties as being a quasi-one-dimensional material [10–13]. The electronic properties of nanotubes are either metallic or semi metallic [14,15], depending on the geometry of how a graphene sheet is rolled up into a tube. Nanotubes present one-dimensional confinement effects and behave as coherent quantum wires and anodes for lithium battery [16–18]. In the previous study, we [19–25] have reported the electrochemical intercalation of lithium into the carbon nanotubes and their by-products. Our results show that carbon nanotubes have large irreversible capacity; one of the main reasons is the electrolyte decomposition and the formation of solid electrolyte interphase. In order to decrease the irreversible capacity, Fong [2] and Laik [26] try to pre-treat the carbon with lithium compounds and can partially prevent the decomposition of the electrolyte, so the raw carbon nanotubes

*Corresponding author. Tel.: +86-731-8836618; fax: +86-731-8879616.
E-mail address: z_h_yang@hotmail.com (Z. Yang).

0925-9635/04/$ - see front matter © 2003 Elsevier B.V. All rights reserved.
doi:10.1016/j.diamond.2003.09.006

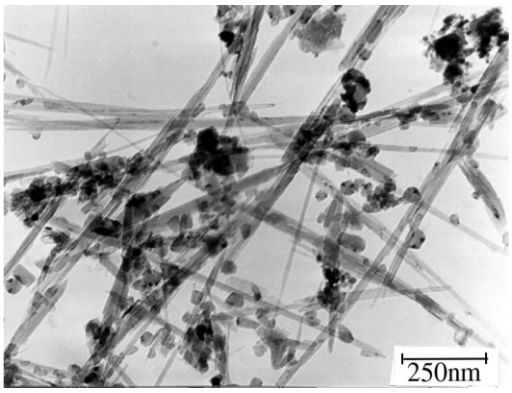

Fig. 1. TEM image of the carbon nanotubes prepared by arc discharge.

were pre-treated by lithium compounds in this paper. The impedance spectroscopies of the raw close and open carbon nanotubes have been reported in Ref. [21]. In this paper we report electrochemical characterization of the raw nanotubes pre-doped with lithium using galvanostatica charge–discharge, cyclic voltammograms and electrochemical spectroscopy.

2. Experimental

The raw carbon nanotubes were prepared under conditions similar to the Krästcher–Hufman [27] technique for the synthesis of fullerenes. An arc was struck between two electrolytic grade (>99%) graphite rods. The rods were initially 15-cm long, the outer diameter of the anode was 8 mm and that of the cathode was 50 mm. The arc was maintained in an atmosphere of 500 Torr helium using a voltage of 18 V DC and a current of 100 A. The carbonaceous materials containing the nanotubes and also nanoparticles were found at the black central core of the deposition formed on the cathodic rod. The sample contains multiwalled carbon nanotubes, anions and amorphous carbon (see Fig. 1). The purity of the carbon nanotubes is above 50% (v/o) as estimated from the Fig. 1. Diameters vary from 5 to 20 nm with a mean value of 15 nm and length are greater than 1 μm, ends of the nanotubes always appear to be capped. The caps have polyhedral shapes with sharp corners (see Ref. [24]). The all nanotubes samples were used without further purification and used the same process.

Carbon nanotubes were opened and filled [28] with lithium compounds by suspending 0.4 g capped nanotubes in 20 g of conc. nitric acid (sp. gr. 1.4) containing 1 g of lithium nitrate and refluxing for 10 h in oil bath at 140 °C. The suspension was allowed to settle and the supernatant solution was decanted. In order to remove the HNO_3 completely, after drying at 100 °C overnight, the resulting insoluble black product was then heated at 300 °C. The tubes containing lithium compound were obtained.

A three-electrode system was applied to use in this study. Lithium sheets were used as reference and counter electrodes. The raw carbon nanotubes pre-doped with lithium were used as working electrode that was a mixture of 85% (weight percent) active material, 10% carbon black and 5% polyvinylidene fluoride (PVDF) binder. The electrode has a geometric area approximately 1.0 cm^2 and total weight of 15–20 mg. The electrode thickness was approximately 0.1 mm. The electrolyte used was a 1 M solution of $LiClO_4$ dissolved in a 50:50 mixture by volume of ethylene carbonate (EC) and dimethyl carbonate (DMC). The cell assembly was carried out under an argon atmosphere in a glove box (UNIlab). The Ar atmosphere was continuously circulated through a purification train containing molecular sieves and the copper metal to remove trace oxygen and water vapor.

The impedance studies were carried out using a PAR model 398 impedance measurement system which was comprised model 5210 lock-in analyzer, a Model 273 potentiostat and an IBM computer. This allowed for the automated measurement of the electrochemical impedance of the cell over the frequency range 100 kHz to 0.01 Hz. The a.c. amplitude was 5 mV peak to peak and the sampling rate of 5 samples per dec. was used.

In the present work, a constant phase element (CPE or Q) is used for equivalent circuits except for resistor, R. The general expression for the admittance of the CPE is

$$Y_{\mathrm{CPE}} = Y_c\omega^n\cos(n\pi/2) + jY_c\omega^n\sin(n\pi/2) \quad (1)$$

where ω is the angular frequency, which is $2\pi f$ with f being frequency and $j=(-1)^{1/2}$. Depending on the n value, the CPE can have a variety of responses, if $n=0$, it represents a resistance with $R=Y_c^{-1}$; if $n=1$, a capacitance with $C=Y_c$, and if $n=0.5$, a Waburg response. The EIS spectra were analyzed using the non-linear least-squares fitting program EQIVCRT developed by Boukamp [29]. The fitting program generates a Chi-square value within the range of 10^{-4} level. The relative S.D. for each parameter, obtained by the fitting program do not exceed 15%. The fitting curves and the experiment data are in good agreement.

3. Results and discussion

The HNO_3 clear solution became a dark yellow color roughly 30 min after the introduction of the carbon nanotubes. The mat did not lose its integrity while in solution even after 24 h after treated with the solution of HNO_3 and $LiNO_3$, more than 90% of the MWNT were opened. From Fig. 2 the result can be seen once the caps of the tube were opened, the shapes with sharp

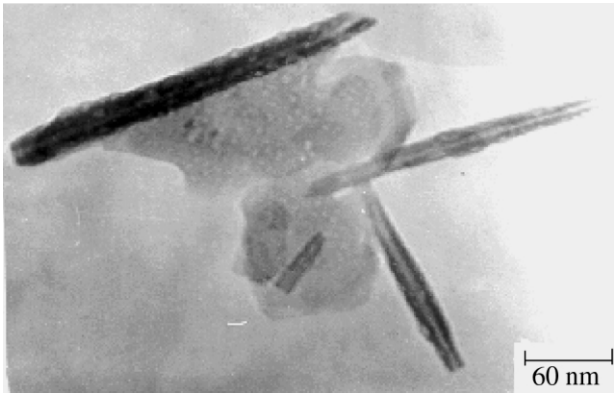

Fig. 2. TEM image of tips of the carbon nanotube with the open end.

corners of caps were disappeared. Chemical treatment with HNO_3 solution revealed a process of opening of the carbon nanotubes from which it was inferred that chemical reactivity is highest at the end caps [28]. Zhou [30] think when the single-wall carbon nanotubes immersed in the HNO_3 solution for a longer period of time, the bundles became disordered and partially exfoliated, isolated nanotubes can be observed, too. For multi-wall carbon nanotubes, the same results can be observed in Fig. 2. With the presence of the $LiNO_3$, the Li-containing compound will be absorbed on the surface of the carbon nanotubes and other forms carbon nanotubes. Meanwhile, according to Tsang's [28] point, the nanotubes will be filled with $LiNO_3$. At the high temperature, the reaction will be occurred:

$$2LiNO_3 \rightarrow 2LiNO_2 + O_2 \quad (2)$$

Partial surfaces of the carbon nanotubes and other forms carbon will be covered with the film of $LiNO_2$.

From the element analysis the results can be obtained that the ⟨Li⟩ content of the sample is 1.8 wt.%, ⟨N⟩ 1.24 wt.%, ⟨O⟩ 1.63 wt.%, so we think the raw carbon nanotubes have been doped with lithium.

The first two charge–discharge curve of the carbon nanotubes is shown in Fig. 3, the current density was 7.5 mA/g. The first discharge curve shows three plateau at 0.9, 0.8 and 0.3 V, the first plateau may be associated with the lithium intercalation into the inner core of the tubes [19], the second plateau may be associated with electrolyte decomposition and causes the formation of a passivate film or a solid electrolyte interphase (SEI) [11] on the carbon surface, in subsequent cycle, Li can insert into the carbon nanotubes reversibly. In Fig. 3, the difference in capacity between the first discharge (1D) and the first charge (1C) is taken to be the irreversible capacity, C_{irr}. The irreversible and reversible capacity for the sample is approximately 500 mAh/g and 200 mAh/g, respectively. The reversible capacity is higher than that of raw carbon nanotubes (125-mAh/g) [20] and the open carbon nanotubes (125-mAh/g) [19].

From Fig. 3 the results can be seen that the first discharge capacity of this sample is 700 mAh g^{-1}, which is nearly equal to the capacity of the opened carbon nanotubes [19]. Also we think that in the process of being treated by HNO_3 and $LiNO_3$ only few of carbon nanotubes were filled with lithium compounds, the others cave cores contain residual gases that might be left from the oxidation process [28]. Meantime Tsang [28] think that less than 1% of the tubes were filled with by his method, our result is consistent with Tsang's conclusion. In the process of the first discharge the lithium can insert into the remnants cores of the carbon nanotubes. Because of the electrostatic attracting of the charged species [19] the lithium cannot de-intercalate from the 'cores' of the carbon nanotubes in the process of the first charge, this is the main source of the irreversible capacity.

Fig. 4a shows the first and second cyclic voltammograms of freshly electrode between 3.0 and 0 V in 1 M $LiClO_4$ + EC: DMC (1:1). On the first cycle voltammogram, reduction current began to flow at ca 1.5 V and two major peaks were observed at ca 0.9 and 0.6 V. The later peak is attributed to solvent decomposition and solid electrolyte interphase (SEI) film formation in this solvent system. Once the film was formed, the Li can intercalate–deintercalate through the film. With the presence of the $LiNO_2$ the solvent decomposition will be partially prevented, so it just shows a trace. The former peak is attributed to the Li intercalation into the inner core of the tube [19]. These peaks disappeared in the second cycle, which mean that the inner core had been filled with lithium and the tube surface was passivated during the first cycle. Redox peaks assigned to lithium intercalation and deintercalation appeared at approximately 0 V and 0.3 V, respectively. In the second cycle, as the potential is scanned from 2.0 V and passes through a potential near 1.1 V increasing cathodic currents are measured. Upon scan reversal near 0 V, the

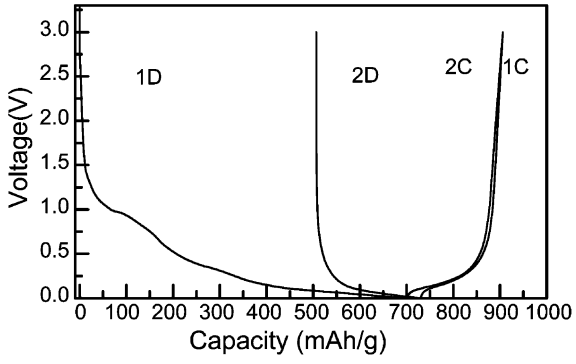

Fig. 3. The discharge–charge curves of the raw carbon nanotubes predoped with lithium.

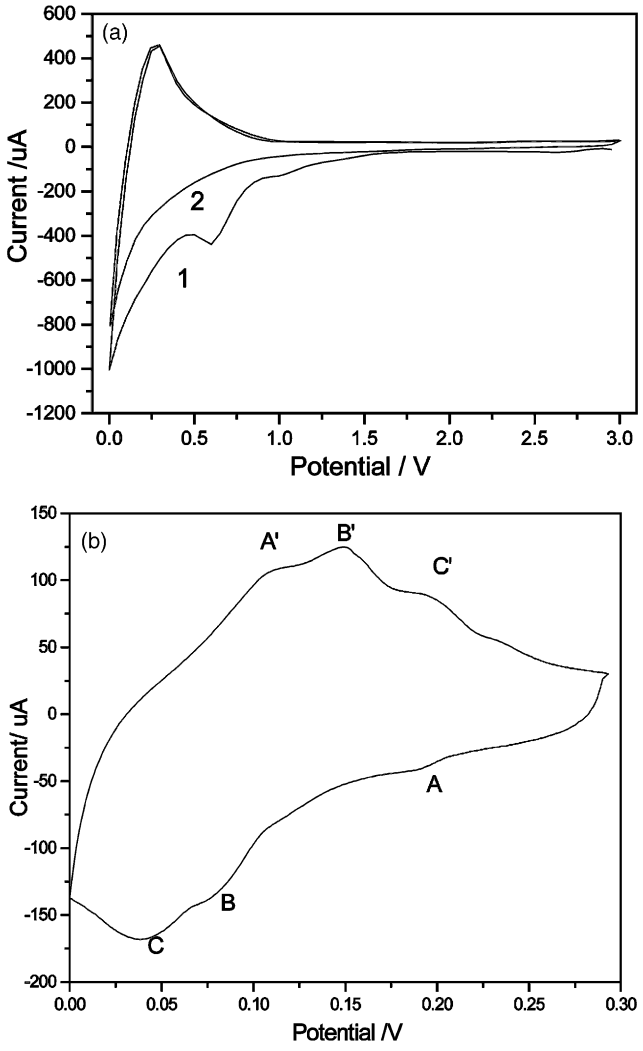

Fig. 4. Cycle voltammograms results of the sample at different scan rate (a) scan rate = 0.1 mV/s and (b) scan rate = 5 μV/s

cathodic current decreases and at a potential near 0.08 V the net current takes on anodic values as the lithium de-intercalate from the carbon nanotubes. After the potential is swept past 0.13 V, the anodic current decreases due to depletion of lithium from the carbon nanotubes and the anodic current falls to small values as the potential approaches 3.0 V after which the cycle is repeated. Because only the tube was in contact with the solution and the sweep rate (0.1 mV/s) was relatively high, so that surface reactions were emphasized.

For Li intercalated in tubes under conditions of slow cyclic voltammetry (5 μV/s), the behavior is shown in Fig. 4b. The three sets of peaks appearing in the voltammograms, the cathodic peaks approximately 190, 85 and 40 mV correspond to the Li insertion, the anodic peaks approximately 200, 150 and 100 mV are their corresponding the reverse Li deintercalation, the areas under the anodic peaks and above the cathodic peaks is the same. It is clear that the charge and discharge curves are reversible. Based on the Li insertion mechanism into graphite, the cathodic peaks in Figure may thus be explained by the staging process (1) dilute phase I to third stage at 0.085 V, (2) third to second stage at ca. 0.040 V and (3) second to 1st stage at more negative potential region.

Impedance spectroscopy may serve as an excellent tool for in situ characterization of the properties of insertion electrodes in general, and lithiated graphite electrodes in particular. The impedance characteristics of pristine electrodes, as well as impedance features of electrodes during cycling, provide very useful information on the stabilization and failure mechanisms of Li-graphite electrodes. The impedance responses shown in Fig. 5a consist of a depressed semicircle in the high frequency range. The depressed semicircle is shown to consist of two arcs. The semicircles at high frequency, which can be modeled by a 'Voigt'-type analog belong

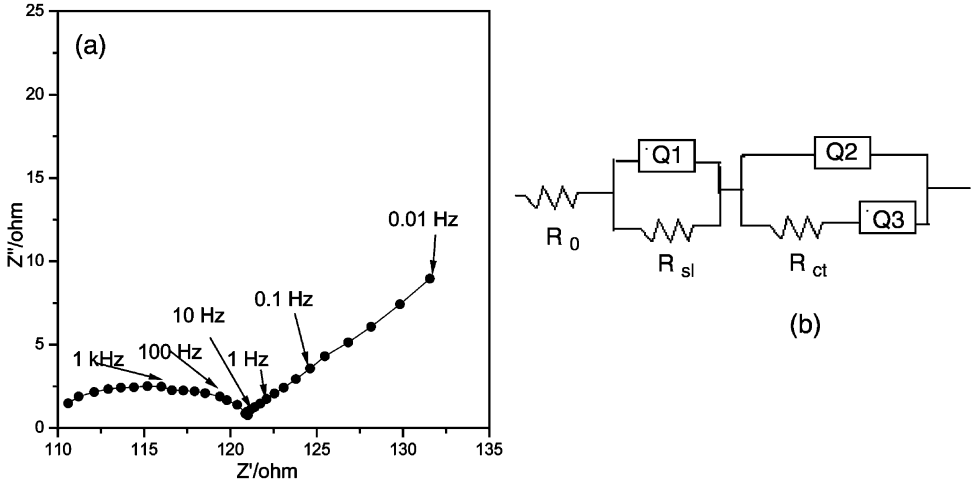

Fig. 5. Impedance spectra of carbon nanotubes pre-doped with lithium (a) and the equivalent circuit.

to Li migration within the surface films. At medium frequency, which are usually semicircular in shape and probably relate to some kind of charge transfer. At lower frequencies, the impedance spectra exhibits a straight line, the straight line can be interpreted as the resistance for the diffusion process of lithium in the carbon nanotubes.

The equivalent circuit presented in Fig. 5b describes the impedance spectra in Fig. 5a. Values obtained for various circuit elements shown in Fig. 5a at different open circuit voltage (OCV) are listed in Table 1. It should be emphasized that all the measurement related to equilibrium potential (under an OCV condition), after the electrodes are cycled galvanostatically six times, showing fully reversible behavior. The equivalent circuit consists of two parallel RQ circuit in series, one for the passive film formation and other for lithium interaction, respectively, as point previously. Three CPEs, Q_1–Q_3, are included in the equivalent circuit. From Table 1 we can see that Q_3 is basically the Warburg impedance with $n \cong 0.5$.

R_0 is ohmic resistance. The R_0 results from three sources: (1) the solution resistance between the working and reference electrode; (2) the wire resistance of the system; (3) the interfacial contact resistance between electrode and electrolyte. No dependence on the electrode potential is seen for R_{sl}, and CPE1 was almost invariant with the electrode potential. (Y_0 and n for the CPE was about and, respectively, with $\mathrm{CPE} = (j\omega)^{-n}/Y_0$). These observations confirm the assignment of R_{sl} to the resistance of Li conduction in the SEI film. In our study, the pristine surface films are comprised of mainly $LiNO_2$. In solutions, the $LiNO_2$ films are replaced by surface species, which relate to complicated reactions between the carbon nanotubes and solution species. The behavior of R_f and C_f probably reflects certain periodical changes in the surface layer (although small in absolute values) as Li de-intercalation proceeds. During the intercalation–deintercalation process, the expansion–contraction of the particles may result in the corresponding change of the surface layer thickness or produce bypassing channels of Li ion migration. However, R_{ct} decreased monotonously when the electrode potential shifted in the cathodic direction. Thus, R_{ct} is confirmed to have its origin at the surface, in addition, the electrode potential dependence can be explained in terms of activation voltage in a charge transfer model, for example, the classical Butler–Volmer formalism, it is, therefore, deduced that R_{ct} certainly reflects the surface charge transfer. The variation in R_{ct} closely mirrored those of the electronic resistance, suggesting a significant electronic contribution to the charge transfer resistance. The other contribution to R_{ct} is ionic in nature, and is due to the resistance to ion transfer across the electrolyte/electrode interface.

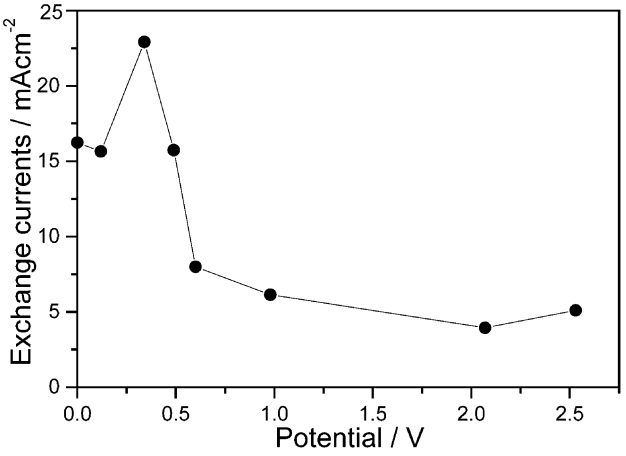

Fig. 6. Variations of exchange currents with the open circuit voltage.

The charge transfer resistance R_{ct}, is related to the exchange currents (i^0) by the equation

$$R_{CT} = RT/(nFi^0) \quad (3)$$

The exchange current densities were calculated using Eq. (3) for various open circuit voltage value as listed in Table 1. The result is shown in Fig. 6. The exchange current densities range between 3 and 24 mA/cm^2.

From the analysis of the impedance spectrum shown in Fig. 5, the diffusion coefficient of Li^+ in the carbon nanotubes electrode can also be determined. As men-

Table 1
Values obtained for simulation of the elements in equivalent circuit shown in Fig. 7 at various open circuit voltage

Open circuit voltage V	R_1 Ω	R_2 Ω	Q1		Q2		Q3	
			YS	n	YS	n	YS	n
0	3.22	1.58	1.19E-3	0.6345	1.55E-4	0.6065	0.210	0.4068
0.12	3.44	1.64	9.86E-4	0.6245	9.51E-4	0.6244	0.190	0.4277
0.34	3.21	1.12	9.48E-4	0.6992	1.89E-3	0.6075	0.105	0.4753
0.49	3.73	1.63	1.09E-3	0.6604	2.02E-3	0.5429	0.101	0.5248
0.60	3.38	3.21	1.35E-3	0.6294	1.64E-3	0.6021	0.076	0.5507
0.98	3.94	4.18	9.64E-4	0.6684	4.16E-3	0.5949	0.012	0.6432
2.07	3.90	6.50	1.28E-3	0.6463	2.53E-3	0.6461	0.002	0.6021
2.53	3.20	5.03	1.48E-3	0.6838	3.95E-3	0.6666	0.002	0.6501

tioned already, the impedance response contain linear portions in the low-frequency range with an angle close to 45°, Warburg impedance Z_w representing the lithium diffusion in the carbon nanotubes can be expressed as

$$Z_w = \frac{C}{\sqrt{j\varpi}} = \frac{C}{\sqrt{2}}\varpi^{-1/2}(1-j) = z' - jz'' \tag{4}$$

where C is constant.

The diffusion of lithium into a single phase in response to a voltage step can be modeled as one-dimensional transport based on Fick second law

$$\frac{\partial C_{\mathrm{Li}}}{\partial t} = D\frac{\partial^2 C_{\mathrm{Li}}}{\partial \chi^2} \tag{5}$$

where x is the distance into the film from the solid-electrolyte interface, C_{Li} is the concentration at x and time t, and D is the chemical diffusion coefficient. The initial and boundary conditions for diffusion into a finite sheet of thickness L, with a constant surface concentration C_s, are:

$$C_{\mathrm{Li}} = C_{\mathrm{O}} \quad 0 \le x \le L \;\; t = 0 \tag{6a}$$

$$C_{\mathrm{Li}} = C_{\mathrm{s}} \quad x = 0 \;\; t > 0 \tag{6b}$$

$$\frac{\partial C_{\mathrm{Li}}}{\partial x} = 0 \quad x = L \;\; t \ge 0 \tag{6c}$$

In this model, D is assumed to be constant over the small concentration range $C_s - C_O$ induced by the voltage step. It is also assumed that Li enters the planar electrode only at the solid-electrolyte interface ($x=0$), that Li cannot leave through the back of the electrode (i.e. the substrate is impenetrable as established by Eq. (6c)) and that the material is single-phase. The D measured in both single-phase and two-phase regions. The D measured in two-phase regions can only be considered to be effective chemical diffusion coefficient. When $\omega \gg 2D/L^2$, Ho [31] think:

$$\frac{\mathrm{d}E}{\mathrm{d}x} = \frac{\sigma n F D^{1/2} A}{V_m} \tag{7}$$

where σ is the preexponential factor of the Warburg impedance, V_m is the molar volume of intercalation host. A the surface area of the electrode. ω the frequency (angle velocity) of a.c., $\mathrm{d}E/\mathrm{d}x$ the differential of the OCV curve, F the Faraday constant, n the value of the diffusion species (Li^+), D the chemical diffusion coefficient of the diffusion species.

The slope of the straight line in the Randles plots (Z vs. $\omega^{-1/2}$ plot) in the low-frequency region is related to σ, but as definite $\mathrm{d}E/\mathrm{d}x$ values were not determined in the low voltage region, according to the equation [32].

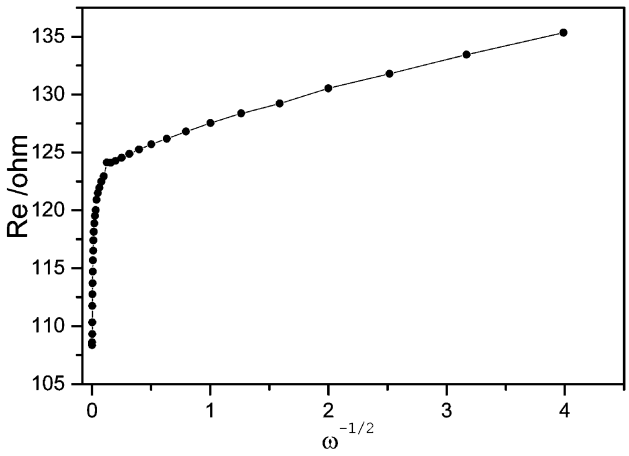

Fig. 7. A typical Randles plot for the carbon nanotubes.

$$\sigma = \frac{1}{nFA\sqrt{2}}\left(\frac{\beta_{\mathrm{O}}}{D_{\mathrm{O}}{}^{1/2}} - \frac{\beta_{\mathrm{R}}}{D_{\mathrm{R}}{}^{1/2}}\right) \tag{8}$$

$$\beta_{\mathrm{O}} = \frac{RT}{nFC_{\mathrm{O}}} \tag{9}$$

$$\beta_{\mathrm{R}} = \frac{RT}{nFC_{\mathrm{R}}} \tag{10}$$

Eq. (8) can be changed into

$$\sigma = RT/\left\{n^2F^2A^{1/2}\left[1/(D_{\mathrm{O}}^{1/2}C_{\mathrm{O}}) + 1/(D_{\mathrm{R}}^{1/2}C_{\mathrm{R}})\right]\right\} \tag{11}$$

Where R is the gas constant, T the absolute temperature and C the concentrations with subscripts representing the oxidant (O) and reductant (R), respectively. Since $D_{\mathrm{O}}{}^{1/2}C_{\mathrm{O}} \gg D_{\mathrm{R}}{}^{1/2}C_R$ under the experimental conditions used in this experiment, Eq. (11) reduces to

$$\sigma = RT/(n^2F^2A^{1/2}D_{\mathrm{R}}{}^{1/2}C_{\mathrm{R}}) \tag{12}$$

The value of C_{R} (mol/cm^3) is calculated from the molar volume of carbon nanotubes and the quantity of lithium intercalated. A typical Randles plot is shown in Fig. 7. The slope of the straight line in the Randles plots (Z vs. $\omega^{-1/2}$ plot) in the low-frequency region is related to σ. The results of the diffusion coefficients are shown in Fig. 8. The diffusion coefficients are in the range of $10^{-22.93}$–$10^{-18.53}$ cm^2/s. The diffusion coefficients shown in Fig. 8 are strongly depending on the open circuit voltage, decreasing with an increase of the open circuit voltage. It showed that the D_{Li} increased as the Li concentration increased. The possible reasons that

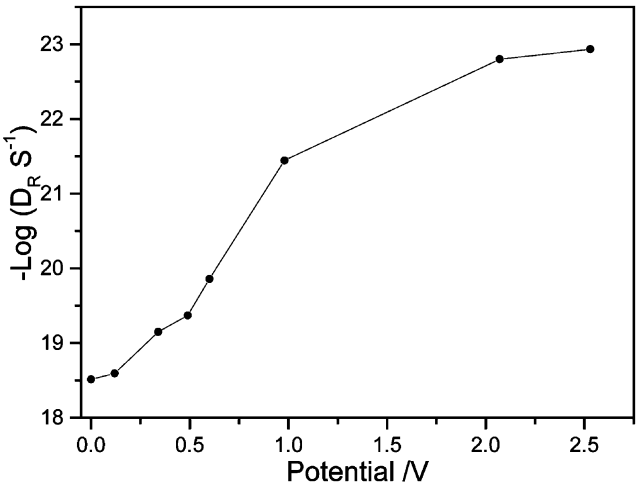

Fig. 8. Variation of diffusion coefficient with the open circuit voltage.

can explain the variations in the diffusion coefficient with the open circuit voltage are controlled by the effective cross-section of the diffusion. We think that the surface of the carbon particles would be covered with a thin film whose chemical composition and transference properties must vary the open circuit voltage, this would cause the difference in the effective cross-section, or in the activity of the diffusion species in the solid phase.

4. Conclusion

The raw carbon nanotubes were synthesized by electric arc method and doped with lithium. Electrochemical impedance spectroscopy was applied for the raw carbon nanotubes pre-doped with lithium during Li-ion insertion in the electrolyte of 1 M $LiClO_4$/EC + DMC. After treated with lithium compounds the solvent decomposition will be partially prevented and the reversible capacity will be increased. The impedance spectra measured consists of a depressed semicircle in the high frequency range and a straight line at low frequency. Obtained spectroscopy were analyzed with an equivalent circuit model. The diffusion coefficients are strongly depending on the open circuit voltage, decreasing with an increase of the open circuit voltage. It showed that the D_{Li} increased as the Li concentration increased. The possible reasons that can explain the variations in the diffusion coefficient with the open circuit voltage are controlled by the effective cross-section of the diffusion.

References

[1] B. Scrosati, Nature 375 (1995) 557.
[2] R. Fong, U. Von Sacken, J.R. Dahn, J. Electrochem. Soc. 137 (1990) 2007.
[3] J.R. Dahn, A.K. Sleignh, H. Shi, J.N. Reimers, Q. Zhong, B.M. Way, Electrochem. Acta 38 (1993) 1179.
[4] T. Zheng, Y. Liu, J.R. Dahn, J. Electrochem. Soc. 142 (1995) 2581.
[5] S. Iijima, Nature 354 (1991) 56.
[6] S. Iijima, Mater. Sci. Eng. B19 (1993) 172.
[7] S. Iijima, Nature 363 (1993) 603.
[8] Y. Fekdman, Science 267 (1995) 222.
[9] P.M. Ajayan, S. Iijima, Nature 358 (1992) 220.
[10] P.M. Ajayan, S. Iijima, Phys. Rev. Lett. 69 (1992) 2689.
[11] D. Aurbach, M.D. Levi, E. Levi, H. Teller, B. Markovsky, G. Salitra, L. Heider, U. Heider, J. Electrochem. Soc. 145 (1998) 3024.
[12] Y. Saito, T. Yoshikawa, M. Okuda, N. Fujimoto, K. Sumiyama, K. Suzuki, et al., J. Phys. Chem. Solid 54 (1993) 1849.
[13] H. Dai, J.H. Hafner, A.G. Rinzler, D.T. Colbert, R.E. Smalley, Nature 384 (1996) 47.
[14] N. Hamada, S. Sawada, A. Oshiyama, Phys. Rev. Lett. 68 (1992) 1579.
[15] R. Satio, M. Fujita, G. Dresselhaus, M.S. Dresselhaus, Appl. Phys. Lett. 60 (1992) 2204.
[16] K. Tanaka, K. Okahara, M. Okada, T. Yamabe, Chem. Phys. Lett. 191 (1992) 469.
[17] T.W. Ebbesen, H.J. Lezec, H. Hiura, J.W. Bennett, H.F. Ghaemi, T. Thio, Nature 382 (1997) 54.
[18] J.W.G. Wilboerm, L.C. Vevema, A.G. Rinzler, R.E. Smalley, C. Dekker, Nature 391 (1998) 59.
[19] Z.H. Yang, H.Q. Wu, Solid State Ionics 143 (2001) 173.
[20] Z.H. Yang, H.Q. Wu, Mater. Chem. Phys. 71 (2001) 7.
[21] Z.H. Yang, H.Q. Wu, Chem. Phys. Lett. 343 (2001) 235.
[22] Z.H. Yang, H.Q. Wu, Chem. Phys. Lett. 343 (2001) 225.
[23] Z.H. Yang, H.Q. Wu, Mater. Lett. 50 (2001) 108.
[24] Z.H. Yang, H.Q. Wu, B. Simard, Electrochem. Commun. 4 (2002) 574.
[25] Z.H. Yang, Z.F. Li, H.Q. Wu, Mater. Lett. 57 (2003) 3160.
[26] B. Laik, F. Gessier, F. Mercier, Electrochimica 44 (1999) 1667.
[27] W. Kratchmer, L.D. Lamb, K. Fortirpoulos, Nature 347 (1990) 354.
[28] Tsang, Nature 372 (1994) 159.
[29] B.A. Boukamp, Solid State Ionics 20 (1986) 31.
[30] C. Bower, A. Kleinhammes, Y. Wu, O. Zhou, Chem. Phys. Lett. 288 (1998) 481.
[31] C. Ho, I.D. Raistrick, R.A. Huggins, J. Electrochim. Acta 38 (1993) 1721.
[32] A.J. Bard, L.R. Faulkner, Electrochemical Methods, Fundamentals and Applications, John Wiley and Sons, New York, 1998.